Volume 1 | Number 1 | Jan 2013 | Pages 1–100

ChemComm

Chemical Communications
www.rsc.org/chemcomm

ROYAL SOCIETY
OF CHEMISTRY

This is an *Accepted Manuscript*, which has been through the Royal Society of Chemistry peer review process and has been accepted for publication.

Accepted Manuscripts are published online shortly after acceptance, before technical editing, formatting and proof reading. Using this free service, authors can make their results available to the community, in citable form, before we publish the edited article. We will replace this *Accepted Manuscript* with the edited and formatted *Advance Article* as soon as it is available.

You can find more information about *Accepted Manuscripts* in the **Information for Authors**.

Please note that technical editing may introduce minor changes to the text and/or graphics, which may alter content. The journal's standard **Terms & Conditions** and the **Ethical guidelines** still apply. In no event shall the Royal Society of Chemistry be held responsible for any errors or omissions in this *Accepted Manuscript* or any consequences arising from the use of any information it contains.

Journal Name

COMMUNICATION

Nanoscale Metal-organic Framework as Highly Sensitive Luminescent Sensor for Fe^{2+} in aqueous solution and living cell

Ye Lu, Bing Yan*, Jin-Liang Liu

We report the exploration of fluorescent nanoscale metal-organic frameworks (nMOF-253s) for highly selective and sensitive detection of Fe^{2+} ion in aqueous solution. Moreover, nMOF-253 with 50 nm is successfully applied in fluorescent bioimaging and intracellular Fe^{2+} sensing in HeLa cell.

Iron species are essential for virtually all organisms for their functions as a cofactor in central cellular process such as respiration, DNA synthesis and repair, ribosome biogenesis, and metabolism, *etc*.[1] In this regard, how to effectively probe iron ion becomes a challenging issue, particularly with the emergence of fluorescent imaging technology.[2] Biological iron is most commonly found in the +2 (ferrous) and +3 (ferric) oxidation states.[3] The sensors for Fe^{3+} are vast and most of them belong to small molecule sensors.[4] Designing a sensor with specificity for ferrous over ferric is difficult due to its propensity for oxidation within aqueous and aerobic conditions.[4] To face this challenge, there are only a few fluorescent sensors selective for Fe^{2+} over Fe^{3+}, pyrene-TEMPO, DansSQ and BPD-Cy-Tpy,[5] all of which are small molecule sensors. Moreover, some flaw is still remained: the probe of pyrene-TEMPO is not completely selective for Fe^{2+}; and DansSQ is only soluble in CH$_3$CN containing 10 % H$_2$O.

Metal-organic frameworks (MOFs), a three dimensional coordination networks with pore, have inherent advantage in selective adsorption and chemical sensing for their large surface area.[6] Nanoscale metal-organic frameworks (nMOFs) have been explored in the biomedical applications.[7] But both nMOFs and nanoscale coordination polymers (NCPs) have not achieved satisfactory result in cell imaging.[7c,8] The phosphor of NCPs or nMOFs almost concentrates around cell wall and fails to be successfully dispersed in cell. So this hinders the further application of nMOFs in cell. In comparison to many new solid luminescent probes[9], the scale of reported NCPs and nMOFs in biomedicine application (close to 100 nm) is obviously larger than the formers (less than 50 nm). Considering the former probes have been successfully applied in the intracellular sensing, it is expected to try nMOFs in intracellular sensing for their intrinsic advantage in sensing.[9a, 9b]

In the present study, we have found that nanoscale MOF-253 (nMOF-253s) has highly sensitive and selective sensing for Fe^{2+}

in aqueous solution. Three kinds of nMOF-253s with different particle sizes (from 300 to 50 nm) are prepared by adjusting the content of base and acid in the reaction system (See experimental details in ESI). The nMOF-253 with 50 nm has been successfully applied in intracellular sensing for Fe^{2+} in HeLa cell. In the structure of MOF-253, a one-dimensional infinite chain of AlO$_6$ corner-sharing octahedral is built by connecting bpydc (bpydc = 2,2'-bipyridine-5,5'-dicarboxylic) linkers to construct rhombic shaped pores (Figure S1).[10] The representative structure of MOF-253 has been isolated by PXRD and a Pawley refinement using the Al(OH)(bpdc) (bpdc^{2-} = 4,4-biphenyldicarboxylate) unit cell parameters in reported work.[10b,11]
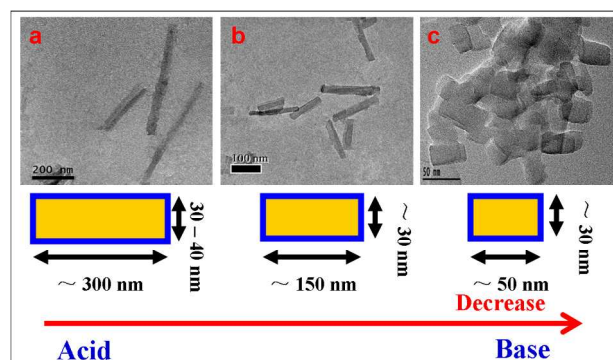

Figure 1. TEM patterns of MOF-253 (α) for (a), MOF-253 (β) for (b) and MOF-253 (γ) for (c).

The syntheses of nMOF-253s are performed under identical conditions except for adding acetic acid or sodium acetate: named as MOF-253 (α) (adding HAc); MOF-253 (β) (adding nothing) and MOF-253 (γ) (adding NaAc). From the transmission electron microscopy (TEM) images (Figure 1), nMOF-253s are a rectangle and its length can be changed by adding acid or base, about 300 nm for MOF-253 (α), 150 nm for MOF-253 (β) and 50 nm for MOF-253 (γ), respectively. But the width has not obviously changed (about 30-40 nm) with the alteration of acid and base. The aspect ratios of MOF-253 (α), MOF-253 (β) and MOF-253 (γ) are 7.5, 5.0 and 1.6, respectively. The selected area electron diffraction patterns (SAED) of nMOF-253s are shown in Figure S2. The size distribution of them is further confirmed by dynamic light scattering (DLS) (Figure S3).

MOF-253 (γ) has the narrowest size distribution among nMOF-253s, which may be due to the smallest aspect ratio. PXRD is shown in the Figure S1. We choose the strangest peak in PXRD patterns (which is located at 6.1 °) to indicate the influence of particle size for PXRD. The full width at half maxima (FWHM) of the peak at 6.1 ° are 0.421 ° for MOF-253 (α), 0.523 ° for MOF-253 (β) and 0.912 ° for MOF-253 (γ), respectively. The smaller particle size can achieve the larger FWHM. The change trend of FWHM corresponds with the results of TEM. The Langmuir surface areas of MOF-253 (α), MOF-253 (β) and MOF-253 (γ) are 1092, 1183 and 1272 m^2/g, respectively (Figure S4).

The excitation spectra of nMOF-253s are obtained by monitoring the emission at 545 nm and are dominated by a broad band centered at about 385-400 nm in the near ultraviolet region, and the emission of nMOF-253s display broad band centered at about 525-625 nm under excitation at 390 nm (Figure S5a). The point of emission spectra in CIE chromaticity diagram is in the region of yellow (Figure S5b). There is some tiny difference on the florescent intensity of nMOF-253s which is due to different particle size: MOF-253 (α) has the strongest fluorescent intensity and MOF-253 (γ) has the weakest fluorescent intensity among nMOF-253s. But there is not too much difference in lifetime and absolute quantum yield (QY) (Figure S6). The lifetime of MOF-253 (α), MOF-253 (β) and MOF-253 (γ) are 7.66, 7.84 and 8.19 μs, respectively. The QY of MOF-253 (α), MOF-253 (β) and MOF-253 (γ) are 35 %, 32 % and 31 %, respectively. In the view of the relative error of QY measurements, the results of QY are coincident with luminescent intensity.[12]
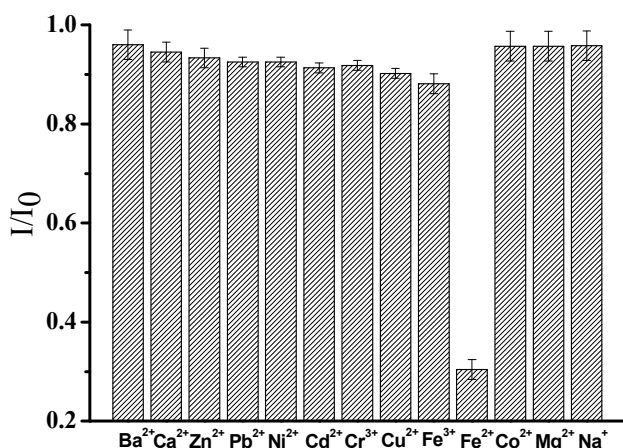

Figure 2. Comparison of the fluorescence intensity of different metal ion incorporated MOF-253 (γ) (50 mg/L) activated in 100 μM M^{X+} (X = 1, 2 or 3) aqueous solution. I and I_0 denote the fluorescence intensity of MOF-253 (γ) with and without metal ions.

The dehydrated MOF-253 (γ) is immersed in aqueous solution containing different of metal ions (Na^+, Ba^{2+}, Ca^{2+}, Mg^{2+}, Pd^{2+}, Zn^{2+}, Cd^{2+}, Ni^{2+}, Co^{2+}, Cu^{2+}, Cr^{3+}, Fe^{2+}, Fe^{3+}) to form the metal ion incorporated MOF-253 (γ) for fluorescent studies. The results show that only Fe^{2+} give significant quenching effect on the fluorescence of MOF-253 (γ), indicating the high selectivity of MOF-253 (γ) for the detection and specific recognition of Fe^{2+} in aqueous solution (Figures 2, S7 and S8). The quenching effect can be quantitatively explained by the Stern–Volmer equation (see ESI). As is shown in Table S1, Fe^{2+} ion has the most significant effect on the fluorescence quenching, the $K_{SV}(Fe^{2+})$ of MOF-253 (γ) is 23333. Meantime, the specific selectivity for recognition of Fe^{2+} also occurs on MOF-253 (α) and MOF-253 (β) (Figure S9). The quench efficiency of MOF-253 (α) is slightly better than MOF-253 (β) and MOF-253 (γ); the $K_{SV}(Fe^{2+})$ of MOF-253 (α) is 26123, which is the biggest among nMOF-253s (Table S1). This maybe indicates that nMOF-253s have the same sensing mechanism for Fe^{2+}.

The fluorescence attenuation may be attributed to a photo-induced electron-transfer (PET) mechanism, like small molecule sensor for Fe^{2+}. The fluorescence emission of MOF-253 is mostly from organic ligands. Free H_2bpydc shows weak fluorescence emission at 555 nm, while MOF-253 displays intense fluorescent emission at 545 nm for forming framework to decreases the intraligand HOMO-LUMO energy gap (Figure S10).[6b] In the reported work, an effective PET process could happened after Fe^{2+} bound to terpyridine.[5c, 13] As a result, the fluorescent intensity of the derivative of terpyridine can be quenched instantaneously; moreover, the PET process based on terpyridine is specific for Fe^{2+} ion over other metal ion.[5c] The same mechanism is likely to work on the MOF-253 whose ligand is the derivative of bipyridine. Taking MOF-253 (γ) as an example, the framework is intact after immersed in Fe^{2+} aqueous solution by checking the PXRD (Figure S11). The coordination between bipyridine and Fe^{2+} is confirmed by X-ray photoelectron spectroscopy (XPS) (Figure S12). The obvious difference between MOF-253 (γ) and MOF-253 (γ) incorporated Fe^{2+} ion on UV-visible diffuse reflectance spectrum (DRS) could indicate the change of electronic structure (Figure S13). Furthermore, this change only occurred on the MOF-253 (γ) incorporated Fe^{2+}. All these facts correspond with the sensing mechanism based on derivative of terpyridine and PET process.[5c] The sensitivity of ligand towards Fe^{2+} is obviously weaker than MOF-253 (γ) (Figure S14). This maybe due to the formation of framework to make the PET based on ligand and analytes more effective.[14] Although MOF-253 (γ) has the weakest fluorescent intensity among nMOF-253s, the smaller scale and the better size distribution endow MOF-253 (γ) unique advantage in biomedical application, especially for intercellular sensing. Hence, the further research focuses on MOF-253(γ).
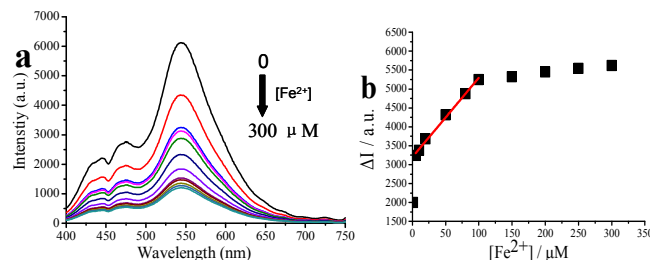

Figure 3. (a) Fluorescence spectra of MOF-253 (γ) (50 mg/L) in aqueous in the presence of various concentrations of Fe^{2+} under excitation at 390 nm. (b) The corresponding calibration curve of MOF-253 (γ) for detecting Fe^{2+} ion. ΔI denotes the quenched fluorescence intensity of MOF-253 (γ). The error bar refers to the standard deviation for triplicate measurements.

Iron species mostly exists in the organisms with the form of coordination complex such as hemin or hematin, an enzyme inhibitor derived from processed red blood cells. We choose hemin to test the special quenching effect of MOF-253 to coordinate ferrous ion. Hemin is Protoporphyrin IX containing a ferric iron ion (Heme B) with a chloride ligand. From Figure S15, the emission intensity of MOF-253 (γ) has obviously weakened after adding hemin aqueous solution (pH = 8.0). The ligand, bpydc, endows MOF-253 with larger pore than parent MIL-53(Al). The coordination complex of Fe^{2+} can easily enter to the voids and react with the bipyridine. MOF-253 (γ) shows a good day-to-day fluorescence stability in aqueous solution and pH-independent fluorescence stability in the pH range of 5−9 (Figure S16). In aqueous solution, the fluorescence of MOF-253(γ) is gradually quenched as the Fe^{2+} concentration increased (Figure 3a). The quenched fluorescence intensity (ΔI) of MOF-253 (γ) has a good linear relationship to the Fe^{2+} concentration ($R^2 = 0.993$) in the concentration range of 5−100 μM Fe^{2+} (Figure 3b). The MOF-253 (γ) probe also gave a low detection limit (3s) of 0.5 μM for Fe^{2+}, which is comparable to or better than those obtained by other fluorescent sensors for Fe^{2+} (Table S2).

The cytotoxicity of MOF-253 (γ) is determined by the reduction activity of methyl thiazolyl tetrazolium (MTT) assay. The viability of untreated HeLa cells is assumed to be 100 %. Upon incubation with different concentration of MOF-253 (γ) (10, 15, 20, 25, 30 and 35 µg/mL) for 24 hrs, more than 85 % of the HeLa cells alive. These results show that MOF-253 (γ) has low toxicity toward cell proliferation (Figure S17).

Figure 4 shows the confocal fluorescence and brightfield images of HeLa cells. As determined by laser scanning confocal microscopy ($\lambda_{ex} = 405$ nm), HeLa cells incubated with MOF-253 (γ) (5 µM) for 3 hrs at 37 °C give intracellular fluorescence (Figure 4a). The overlay of fluorescence and brightfield images reveal that the fluorescence signals are almost localized in the perinuclear region of the cytosol. The subcellular distribution of MOF-253 (γ) indicates that MOF-253 (γ) is internalized into the living cells from the growth medium. This is further confirmed by Z-scan fluorescent imaging of living HeLa cells incubated with MOF-253 (γ) (Figure S18). The clear fluorescence signal also explains the integrity of MOF-253(γ) because free H_2bypdc cannot emit green-yellow light under 405nm. (The excitation of free H_2bypdc is a sharp band located at 361 nm under monitoring emission at 545 nm from Figure S10.)
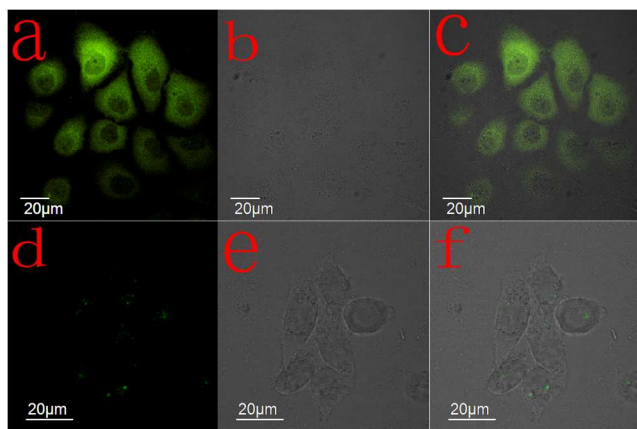

Figure 4. Confocal fluorescence and brightfield images of HeLa cells. (a) fluorescent image, (b) brightfield image, (c) overlay image of HeLa cells stained with 5 µM MOF-253 (γ) for 3 hrs at 37 ºC; (d) fluorescence image, (e) brightfield image, (f) overlay image of HeLa cells incubated with 5 µM MOF-253 (γ) and then supplemented with 50 µM $FeCl_2$ in the growth media for 1 hr at 37 ºC ($\lambda_{ex} = 405$ nm).

When the cells incubated with MOF-253(γ) are supplied with 50 µM $FeCl_2$ in the growth medium for 1 h at 37 °C, a significant fluorescence quenching from the intracellular region can be observed (Figure 4 (a–f)). Brightfield measurements with or without the treatment with Fe^{2+} ion confirm that the cells were viable throughout the imaging experiments. For further comparison, the cells supplemented with $FeCl_3$ have been done in the same experiment condition (Figure S19). It can be observed that the fluorescence from the intracellular region is not obviously changed in comparison to untreated sample with Fe^{3+} ion. The consistency of the experiment results in cell and aqueous proves the sensing of MOF-253 (γ) for Fe^{2+} ion in cell is effective.

In summary, we discover that MOF-253 has outstanding fluorescent quenching specificity for Fe^{2+} ion. Three kinds of nMOF-253s from 300 to 50 nm have been prepared by adjusting the content of base and acid in the reaction system. Moreover, MOF-253 (γ) could be successfully introduced into HeLa cell and applied in intracellular ferrous sensing. Our investigation highlights the potential value of nanoscale MOFs as a novel platform for designing luminescent hybrid biomaterial with bioimaging and intracellular sensing.

Notes and references

Department of Chemistry, Tongji University, Shanghai 200092, P. R. China. Fax: (+86) 21-65982287; E-mail: byan@tongji.edu.cn

1 (*a*) J. Reinking, M. M. S. Lam, K. Pardee, H. M. Sampson, S. Y. Liu, P. Yang, S. Williams, W. White, G. Lajoie, A. Edwards and H. M. Krause, *Cell*, 2005, **122**, 195; (*b*) A. A. Salahudeen, J. W. Thompson, J. C. Ruiz, H. W. Ma, L. N. Kinch, Q. M. Li, N. V. Grishin and R. K. Bruick, *Science*, 2009, **326**, 722;

2 (*a*) R. E. Fleming, *Cell Metab.*, 2009, **9**, 211; (*b*) N. Takahashi-Makise, D. M. Ward and J. Kaplan, *Nat. Chem. Biol.*, 2009, **5**, 874.

3 E. L. Que, D. W. Domaille and C. J. Chang, *Chem. Rev.*, 2008, **108**, 4328.

4 L. M. Hyman and K. J. Franz, *Coordin. Chem. Rev.*, 2012, **256**, 2333;

5 (*a*) J. L. Chen, S. J. Zhuo, Y. Q. Wu, F. Fang, L. Li and C. Q. Zhu, *Spectrochim Acta A*, 2006, **63**, 438; (*b*) L. Praveen, M. L. P. Reddy and R. L. Varma, *Tetrahedron Lett.*, 2010, **51**, 6626; (*c*) P. Li, L. B. Fang, H. Zhou, W. Zhang, X. Wang, N. Li, H. B. Zhong and B. Tang, *Chem-Eur. J.*, 2011, **17**, 10520.

6 (*a*) L. E. Kreno, K. Leong, O. K. Farha, M. Allendorf, R. P. Van Duyne and J. T. Hupp, *Chem. Rev.*, 2012, **112**, 1105; (*b*) Y. J. Cui, Y. F. Yue, G. D. Qian and B. L. Chen, *Chem. Rev.*, 2012, **112**, 1126; (*c*) J. Jia, F. J. Xu, Z. Long, X. D. Hou and M. J. Sepaniak, *Chem. Commun.*, 2013, **49**, 4670; (*d*) L. Chen, K. Tan, Y. Q. Lan, S. L. Li, K. Z. Shao and Z. M. Su, *Chem. Commun.*, 2012, **48**, 5919; (*e*) B. L. Chen, L. B. Wang, Y. Q. Xiao, F. R. Fronczek, M. Xue, Y. J. Cui and G. D. Qian, *Angew. Chem. Int. Edit.*, 2009, **48**, 500; (*f*) W. S. Liu, T. Q. Jiao, Y. Z. Li, Q. Z. Liu, M. Y. Tan, H. Wang and L. F. Wang, *J. Am. Chem. Soc.*, 2004, **126**, 2280; (*g*) B. Zhao, X. Y. Chen, P. Cheng, D. Z. Liao, S. P. Yan and Z. H. Jiang, *J. Am. Chem. Soc.*, 2004, **126**, 15394.

7 (*a*) P. Horcajada, R. Gref, T. Baati, P. K. Allan, G. Maurin, P. Couvreur, G. Ferey, R. E. Morris and C. Serre, *Chem. Rev.*, 2012, **112**, 1232; (*b*) P. Horcajada, T. Chalati, C. Serre, B. Gillet, C. Sebrie, T. Baati, J. F. Eubank, D. Heurtaux, P. Clayette, C. Kreuz, J. S. Chang, Y. K. Hwang, V. Marsaud, P. N. Bories, L. Cynober, S. Gil, G. Ferey, P. Couvreur and R. Gref, *Nat. Mater.*, 2010, **9**, 172; (*c*) K. M. L. Taylor-Pashow, J. Della Rocca, Z. G. Xie, S. Tran and W. B. Lin, *J. Am. Chem. Soc.*, 2009, **131**, 14261.

8 (*a*) D. M. Liu, R. C. Huxford and W. B. Lin, *Angew. Chem. Int. Edit.* 2011, **50**, 3696; (*b*) J. D. Rocca, D. M. Liu and W. B. Lin, *Accounts Chem. Res.*, 2011, 44, 957.

9 (*a*) X. Michalet, F. F. Pinaud, L. A. Bentolila, J. M. Tsay, S. Doose, J. J. Li, G. Sundaresan, A. M. Wu, S. S. Gambhir and S. Weiss, *Science*, 2005, **307**, 538; (*b*) J. Zhou, Z. Liu and F. Y. Li, *Chem. Soc. Rev.*, 2012, 41, 1323; (*c*) J. L. Liu, Y. Liu, Q. Liu, C. Y. Li, L. N. Sun and F. Y. Li, *J. Am. Chem. Soc.*, 2011, **133**, 15276; (*d*) Q. Liu, T. S. Yang, W. Feng and F. Y. Li, *J. Am. Chem. Soc.*, 2012, **134**, 5390; (*e*) Q. Liu, B. R. Yin, T. S. Yang, Y. C. Yang, Z. Shen, P. Yao and F. Y. Li, *J. Am. Chem. Soc.*, 2013, **135**, 5029.

10 (*a*) S. M. Cohen, *Chem. Rev.*, 2012, **112**, 970; (*b*) E. D. Bloch, D. Britt, C. Lee, C. J. Doonan, F. J. Uribe-Romo, H. Furukawa, J. R. Long and O. M. Yaghi, *J. Am. Chem. Soc.*, 2010, **132**, 14382.

11 I. Senkovska, F. Hoffmann, M. Froba, J. Getzschmann, W. Bohlmann and S. Kaskel, Micropor. Mesopor. Mat., 2009, 122, 93.

12 L. D. Carlos, R. A. Ferreira, Z. Bermudez Vde, S. J. Ribeiro, *Adv. Mater.,* 2009, **21**, 509.

13 A. P. de Silva, H. Q. N. Gunaratne, T. Gunnlaugsson, A. J. M. Huxley, C. P. McCoy, J. T. Rademacher and T. E. Rice, *Chem. Rev.*, 1997, **97**, 1515.

14 (*a*) S. R. Zhang, D. Y. Du, J. S. Qin, S. J. Bao, S. L. Li, W. W. He, Y. Q. Lan, P. Shen and Z. M. Su, *Chem-Eur. J.*, 2014, **20**, 3589; (*b*) Y. Y. Bao, Q. B. Li, B. Liu, F. F. Du, J. Tian, H. Wang, Y. X. Wang and R. K. Bai, *Chem. Commun.*, 2012, **48**, 118.